
東京大学 生産技術研究所
北條 博彦

化学生命工学専攻
有機機能材料科学特論II

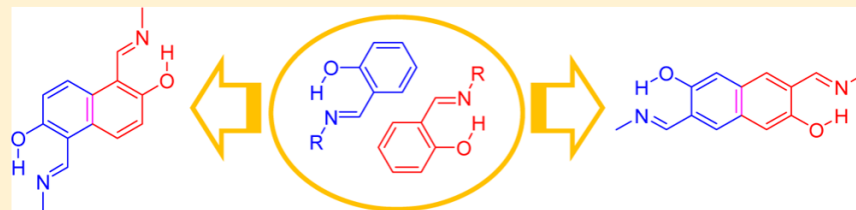
Mutual Interference between Intramolecular Proton Transfer Sites through the Adjoining π -Conjugated System in Schiff Bases of Double-Headed, Fused Salicylaldehydes

Hirohiko Houjou,* Hajime Shingai, Keisuke Yagi, Isao Yoshikawa, and Koji Araki

Institute of Industrial Science, The University of Tokyo, 4-6-1 Komaba, Meguro-ku, Tokyo 153-8505, Japan

J. Org. Chem. **78** (2013) 9021-9031.

ABSTRACT: We synthesized two constitutionally isomeric bis(iminomethyl)-2,6-dihydroxynaphthalenes, namely, α,α -diimines **1** and β,β -diimines **2**, which can be formally represented as fused salicylaldimines with resonance-assisted hydrogen-bonding sites. Spectroscopic data show that the OH/OH, NH/OH, and NH/NH forms of **1** were in equilibrium in solution and that the proportion of the NH-bearing tautomers increased as the solvent polarity increased. The UV spectra of thin solid films of **1** with various types of hydrogen-bonding networks differed from one another, and the spectral profiles were markedly temperature dependent, whereas the spectra of **1** in the molten state showed quite similar profiles. In contrast, **2** existed predominantly as the OH/OH form irrespective of the solvent polarity or crystal packing. Quantum chemical calculations suggest that the difference between the probabilities of intramolecular proton transfer in **1** and **2** can be explained in terms of the interplay between the resonance-assisted hydrogen-bonding sites and the adjoining π -conjugated system.



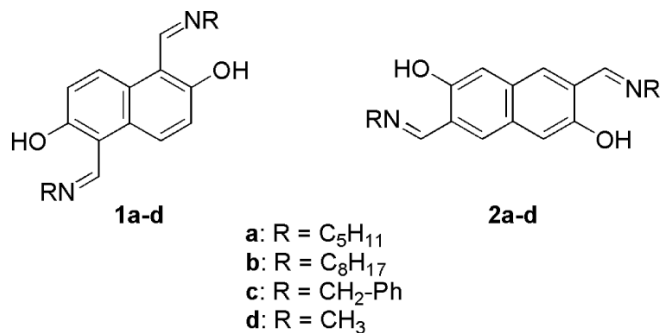
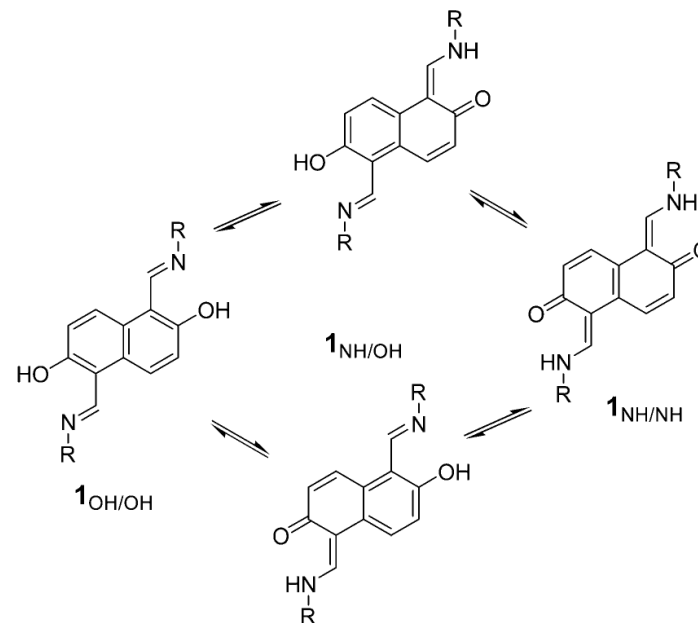
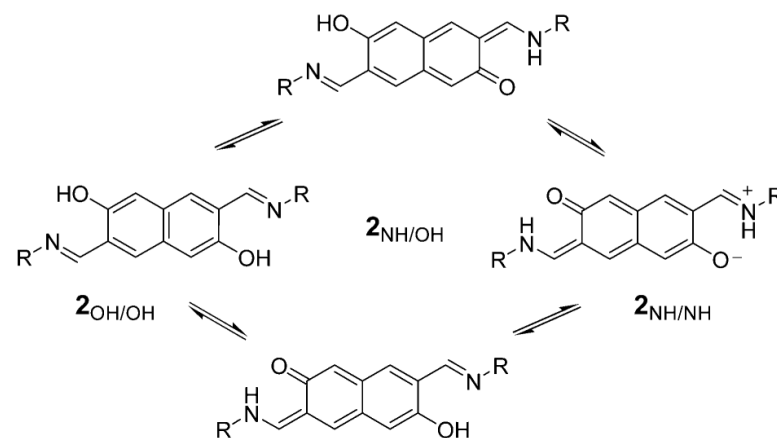
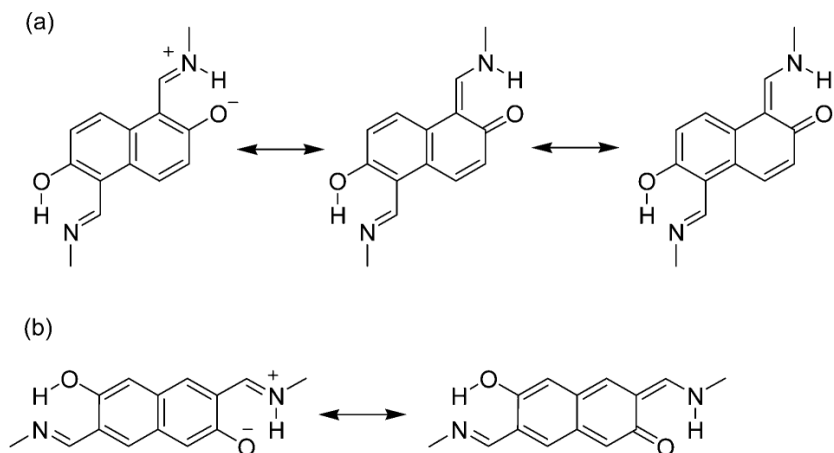


Figure 1. Structures of α,α -diimines **1** and β,β -diimines **2**.

Scheme 1. Possible Tautomers of α,α -Diimines **1** and β,β -Diimines **2**



Scheme 2. Resonance Hybridization Schemes for the NH/OH Forms of (a) α,α -Diimines **1** and (b) β,β -Diimines **2**



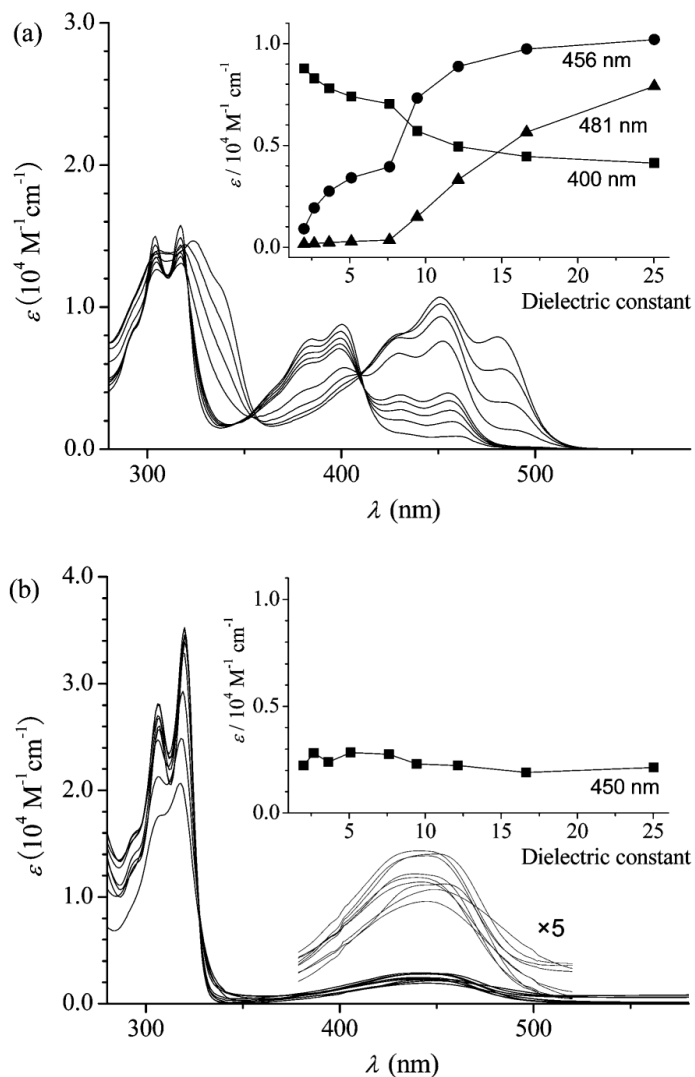


Figure 2. UV-vis absorption spectra of (a) **1b** and (b) **2b** in methylcyclohexane, tetrahydrofuran, ethanol, 75/25, 50/50, and 25/75 mixtures of methylcyclohexane and tetrahydrofuran, and 75/25, 50/50, and 25/75 mixtures of tetrahydrofuran and ethanol. Each inset shows the absorptivity at selected wavelengths as a function of the dielectric constant of the solvents used.

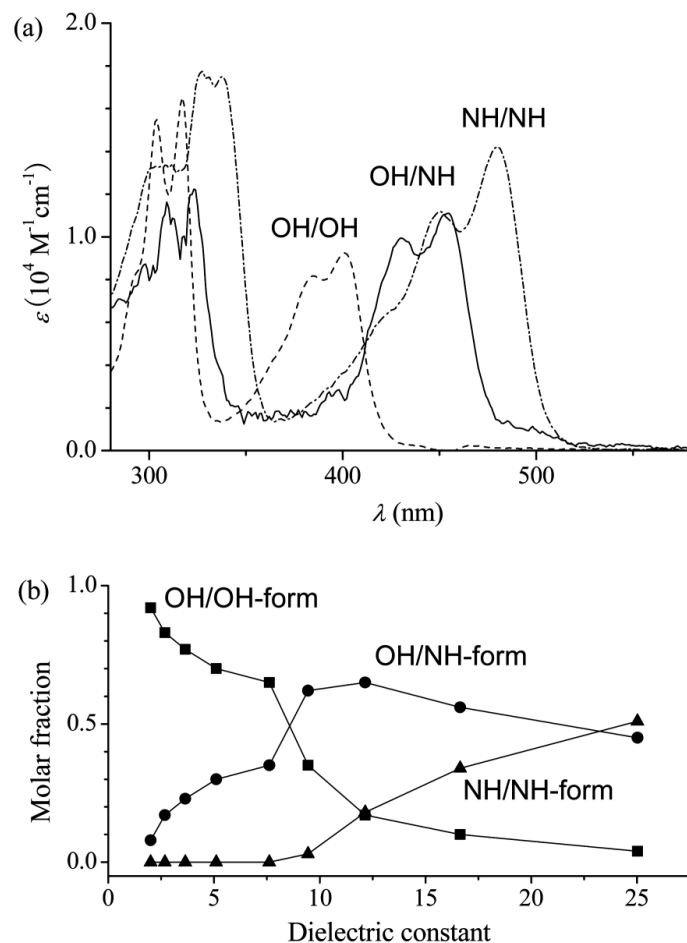


Figure 3. (a) Ideal spectra of the OH/OH, NH/OH, and NH/NH forms of **1b**. (b) Solvent dependence of the molar fraction of each tautomer, calculated on the basis of the ideal spectra.

In contrast, in pure ethanol ($\epsilon = 25$), **1b**_{NH/NH} was the major component and the **1b**_{OH/OH}/**1b**_{NH/NH} and **1b**_{NH/OH}/**1b**_{NH/NH} population ratios were 0.08 and 0.88, respectively. The difference in solvent composition dependence between **1b**_{NH/OH} and

Table 1. Energies of Tautomers of Aldimines Calculated at the B3LYP/6-311G Level**

	energy (kJ/mol)		λ_{\max} (nm)		$\langle \text{HOMA} \rangle^a$	
	$\epsilon = 1$	$\epsilon = 25$	$\epsilon = 1$	$\epsilon = 25$	$\epsilon = 1$	$\epsilon = 25$
1 _{OH/OH}	(0.0)	(0.0)	360	358	0.70	0.70
1 _{NH/OH}	+6.9	−7.7	396	396	0.39	0.46
1 _{NH/NH}	+20.4	−9.9	441	446	0.00	0.19
2 _{OH/OH}	(0.0)	(0.0)	431	413	0.78	0.77
2 _{NH/OH}	+45.1	+21.2	599	578	0.36	0.60
2 _{NH/NH}	+89.8	+51.9	950	912	0.67	0.66
3 _{OH}	(0.0)	(0.0)	290	286	0.98	0.98
3 _{NH}	+22.8	+4.2	355	360	0.19	0.46

^aHarmonic oscillator model of aromaticity index averaged over the two six-membered rings.

$$\text{HOMA} = 1 - \frac{\alpha}{n} \sum_{i=1}^n (R_{\text{opt}} - R_i)^2$$

mol, respectively; as a result, the relative stabilities of the two tautomers were opposite those observed under in vacuo conditions. We calculated the energetic difference between **1**_{NH/OH} and **1**_{NH/NH} to be 2.18 kJ/mol, and from this value, we calculated the **1**_{NH/OH}/**1**_{NH/NH} population ratio to be 0.83 (at 298 K) when we correctly included the statistical weight of the tautomers. The **1**_{OH/OH}/**1**_{NH/NH} population ratio was calculated to be 0.02. These values were in good agreement with the observed values (0.88 and 0.08, respectively); therefore, we concluded that this level of calculation was sufficient.

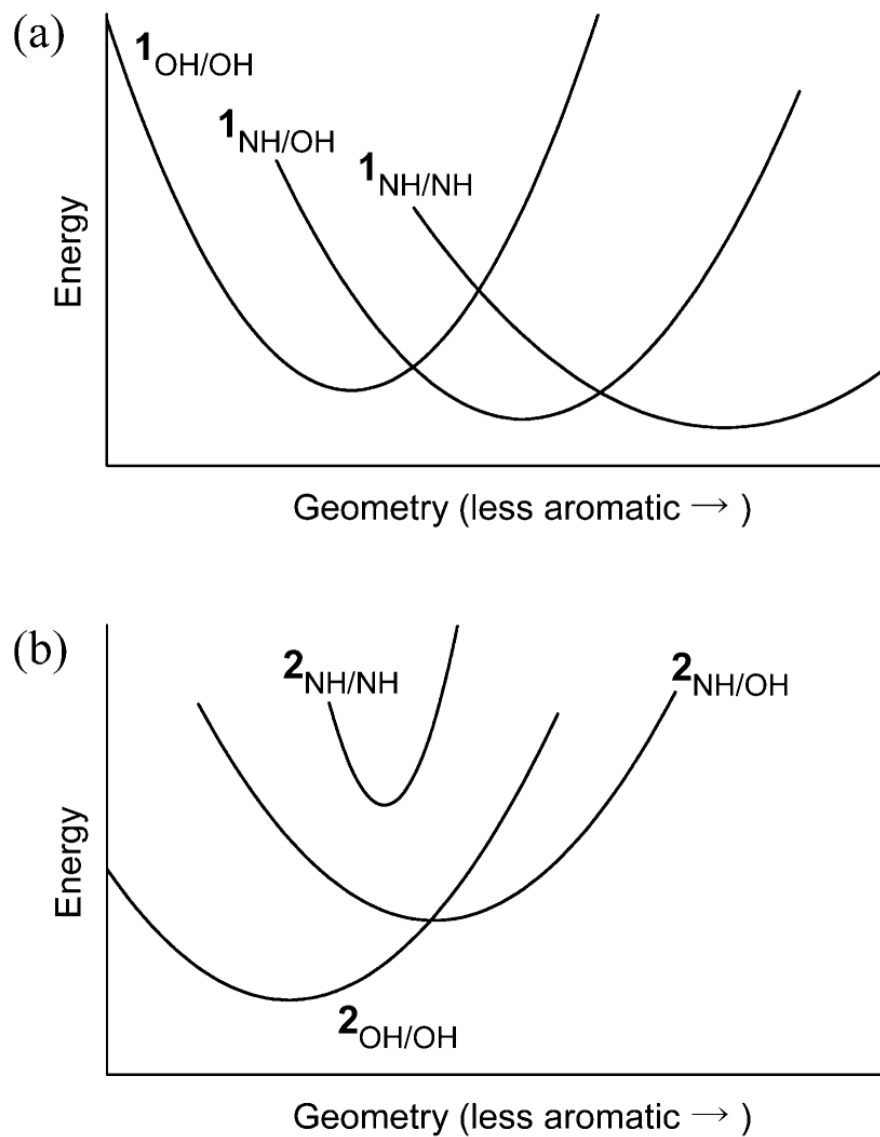
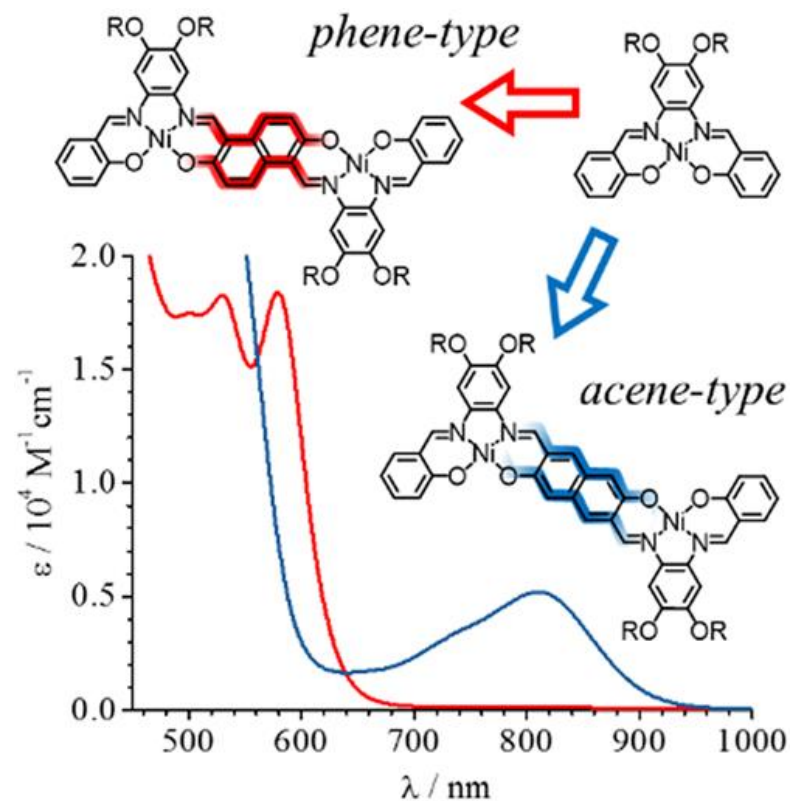


Figure 10. Approximate quadratic potential curves for the tautomers of (a) 1 and (b) 2. Energy is plotted against a geometrical parameter related to the loss of aromaticity.

Effects of interaction between the chelate rings and π -conjugated systems in fused salphen complexes on UV-Vis-NIR spectra

Hirohiko Houjou | Keisuke Yagi | Isao Yoshikawa | Toshiki Mutai | Koji Araki

J. Phys. Org. Chem. **30** (2017) e3635.


Abstract

Dinuclear (Zn_2 , Ni_2 , and NiZn) complexes of fused salphen with acene-type annelation were synthesized from 3,7-diformyl-2,6-dihydroxynaphthalene. The spectroscopic properties of these complexes were compared with those of their constitutional isomers with phene-type annelation. The acene-type complexes exhibited a characteristic absorption band in the near-infrared region that showed a noticeable solvent effect. Time-dependent density functional theory calculations suggested that the absorption arose from a $\pi \rightarrow \pi^*$ transition localized at the naphthalene ring, which was perturbed by the adjoining chelate rings. Effects of the connection topology in the fused salphen complexes are discussed by comparison with those of polycyclic aromatic hydrocarbons.

KEYWORDS

aromaticity, conjugation, density functional calculations, isomer effect, near-infrared absorption, polycyclic aromatic hydrocarbon, Schiff bases, transition metal, UV-Vis spectroscopy

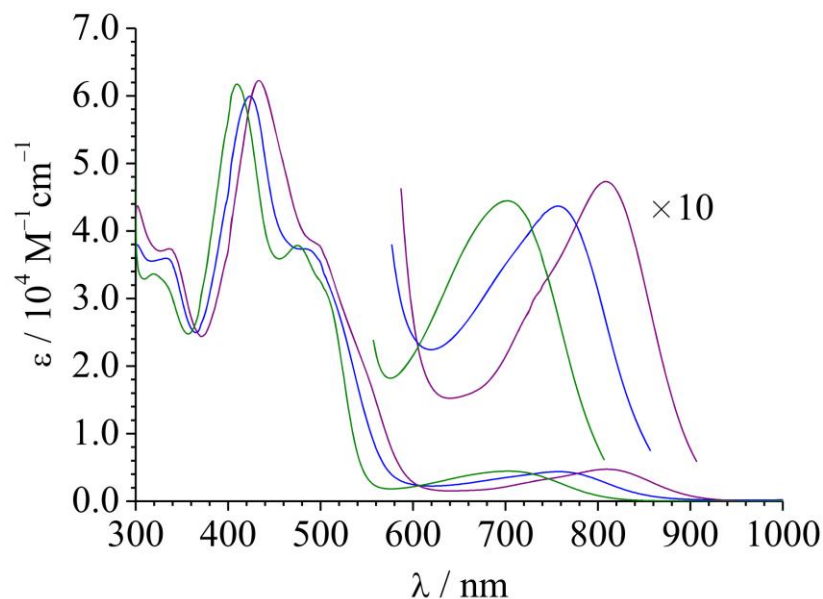


FIGURE 2 UV-visible-near-infrared spectra of $\text{Zn}_2\text{L}^\beta$ (green), $\text{Ni}_2\text{L}^\beta$ (violet), and NiZnL^β (blue) in pyridine ($1 \times 10^{-5}\text{M}$)

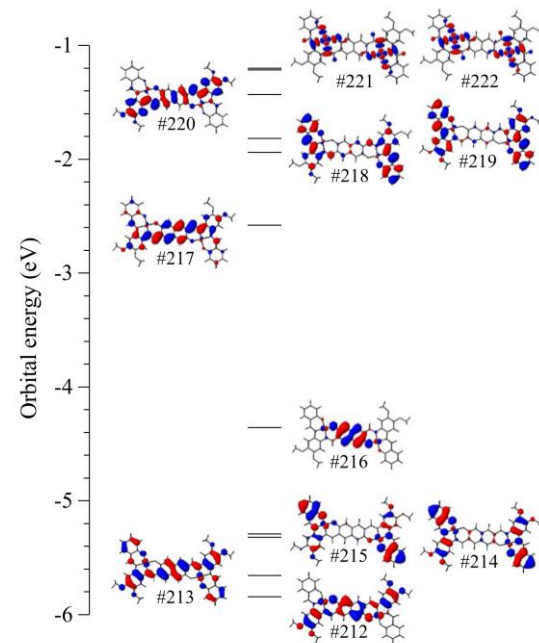


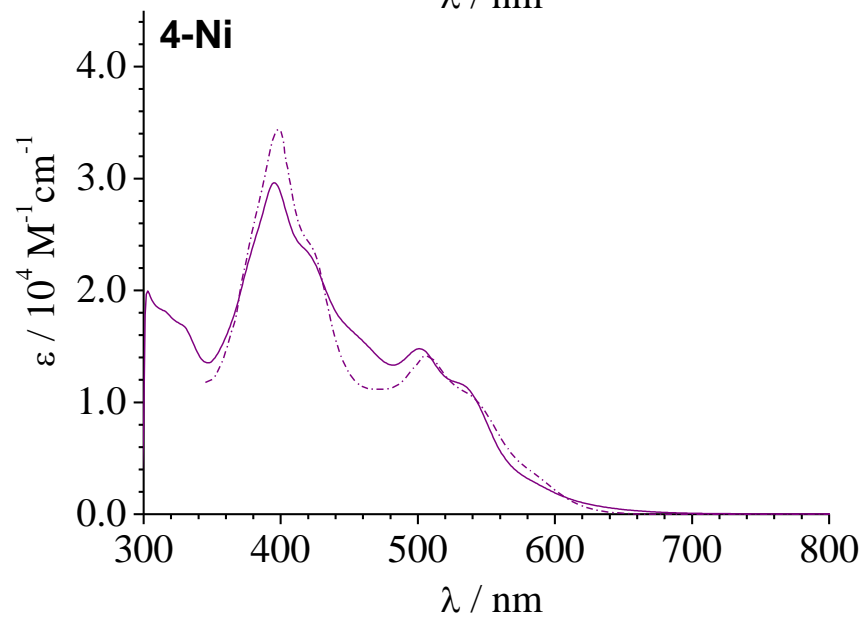
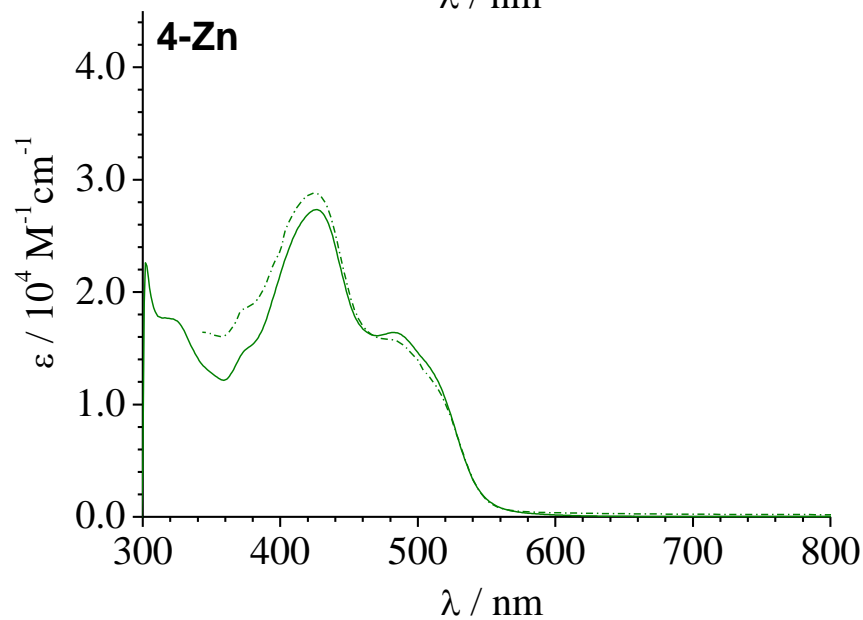
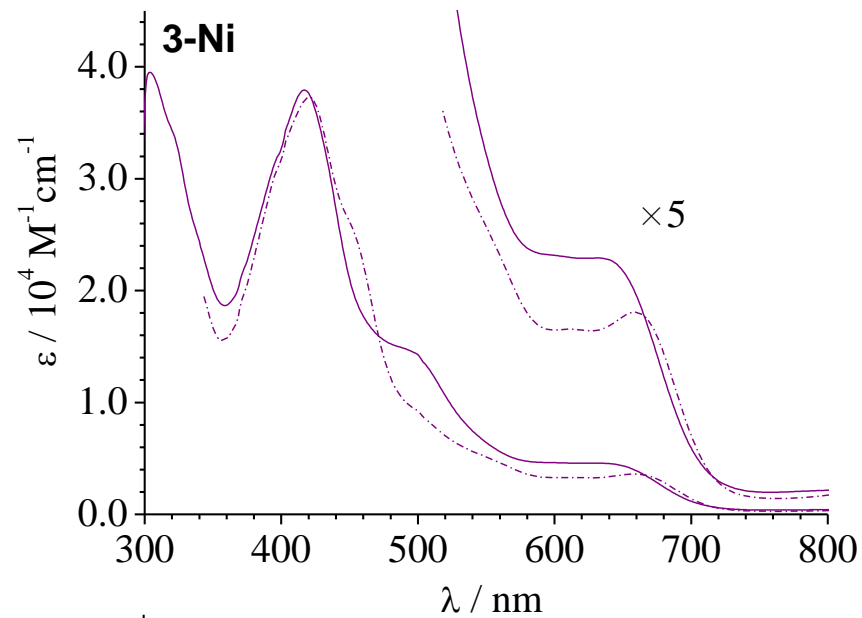
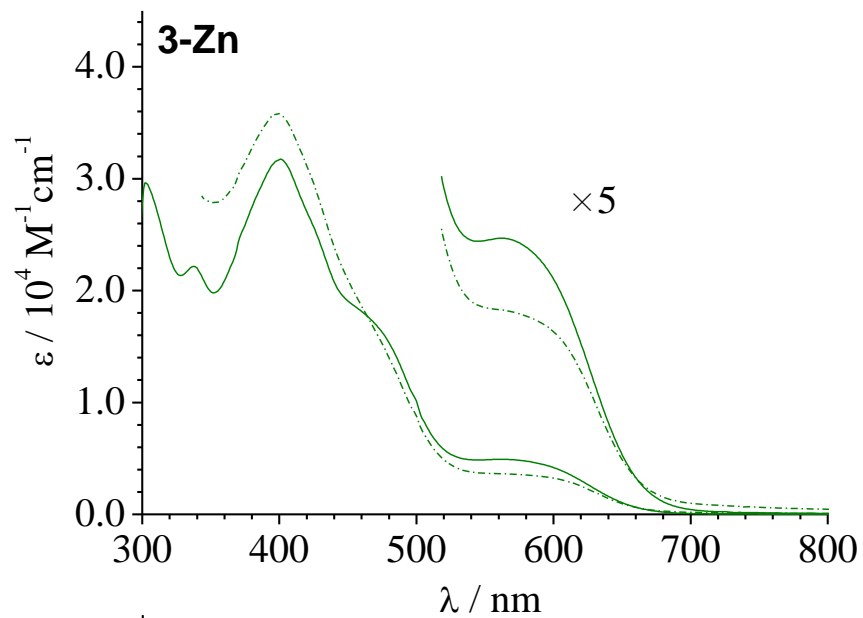
FIGURE 4 Orbital energy diagram and visualization of the near-highest occupied molecular orbital and near-lowest unoccupied molecular orbital of $\text{Ni}_2\text{L}^\beta$

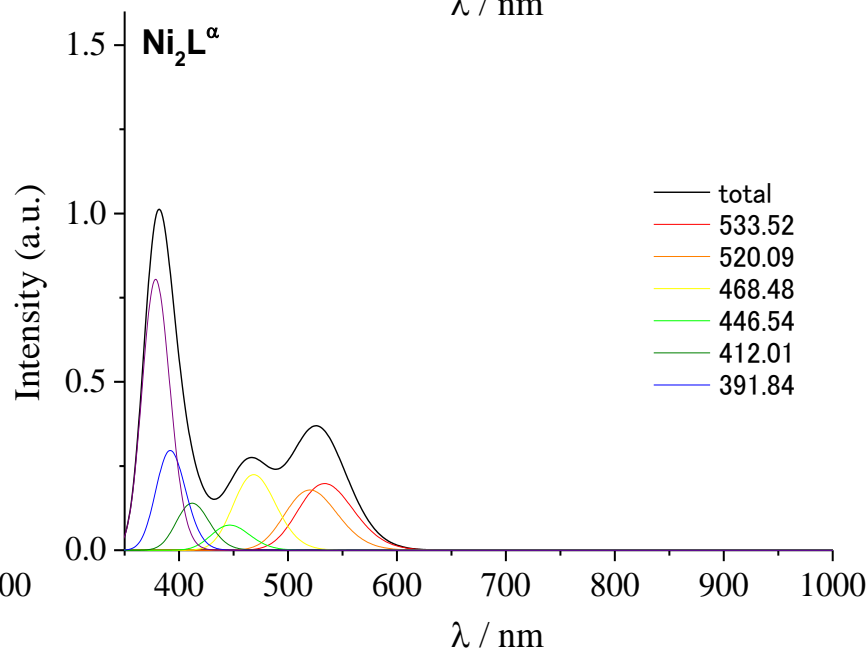
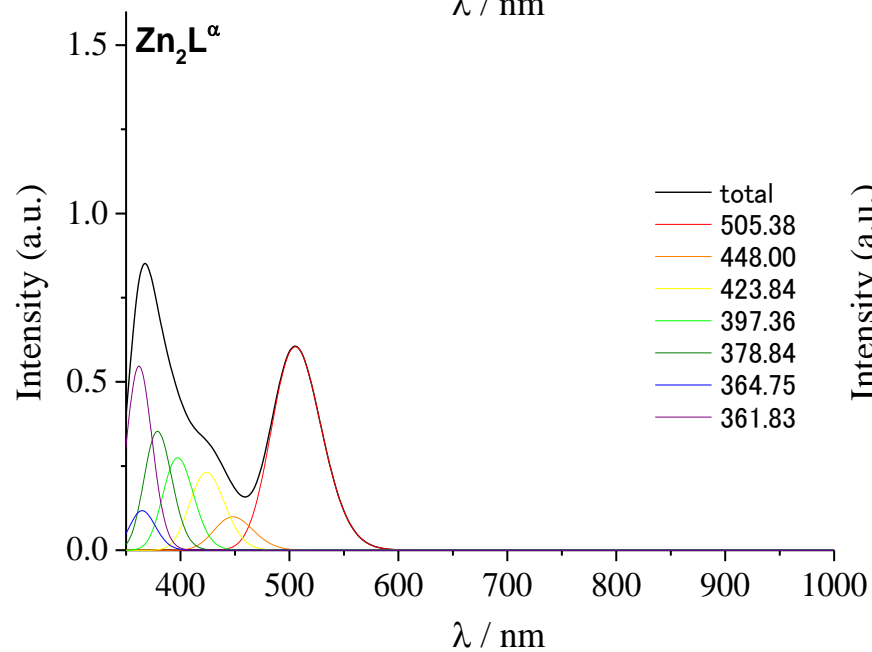
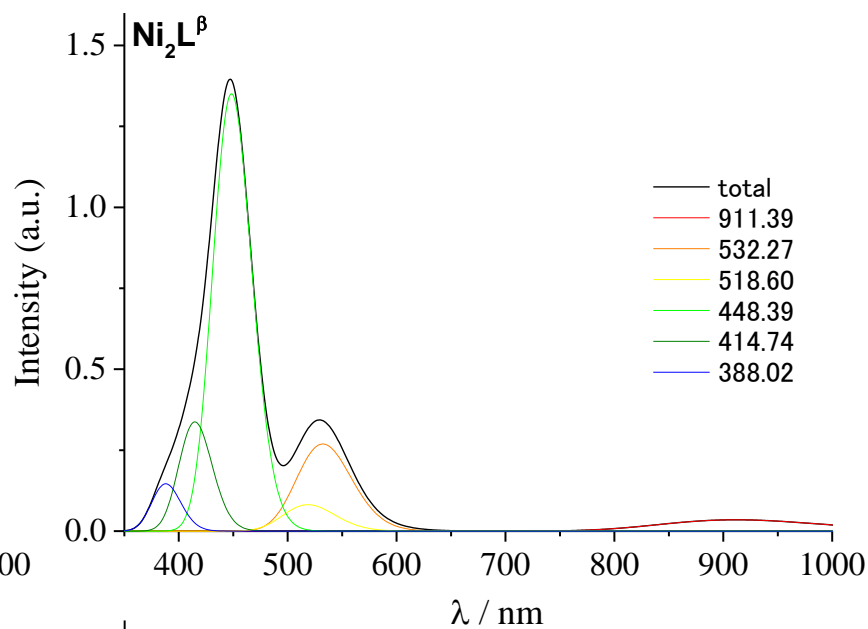
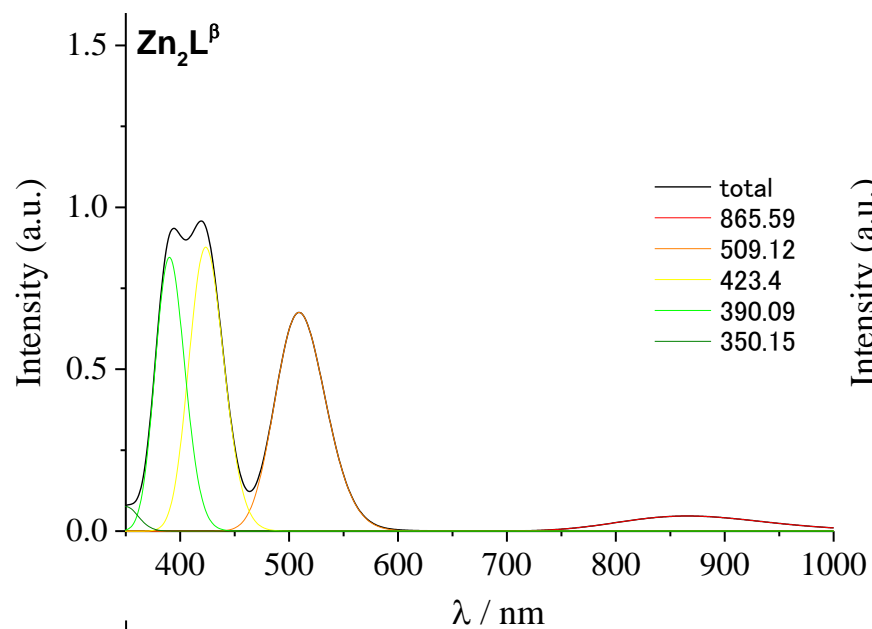
TABLE 1 Selected results from the TD-DFT calculations for acene-type fused salphen complexes

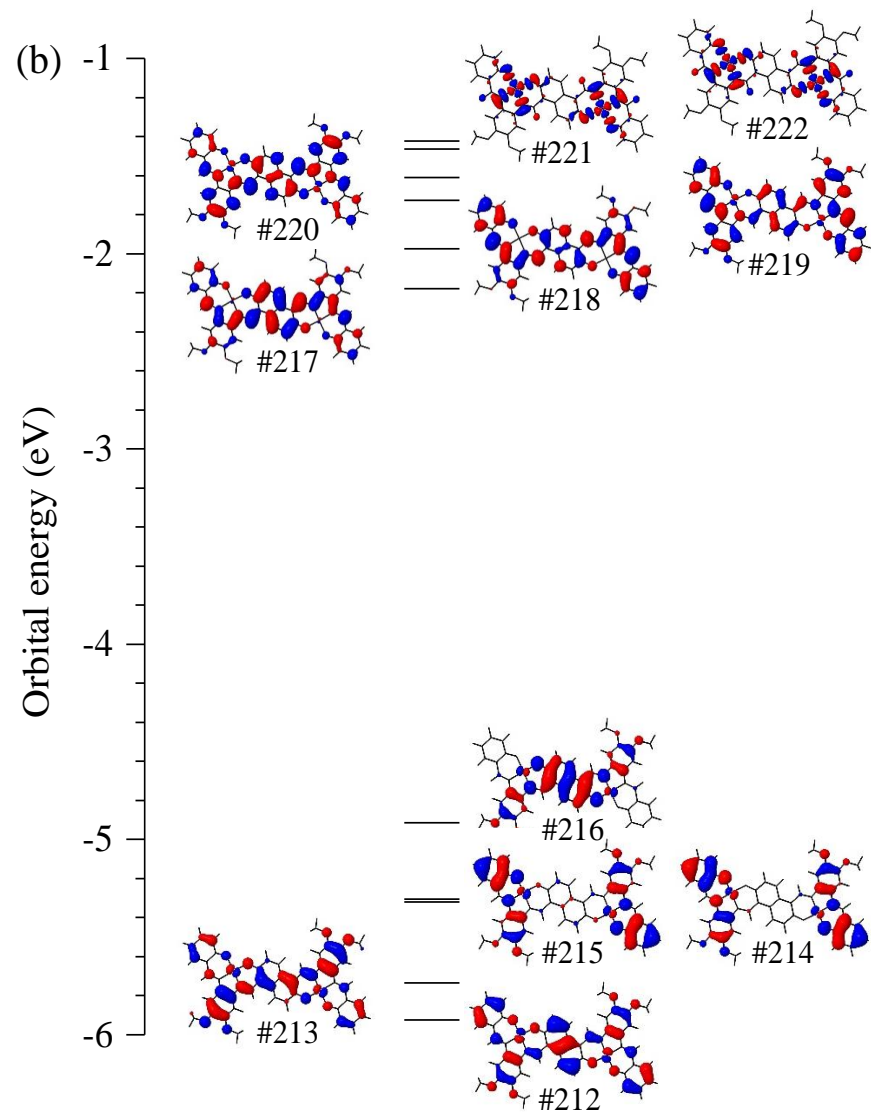
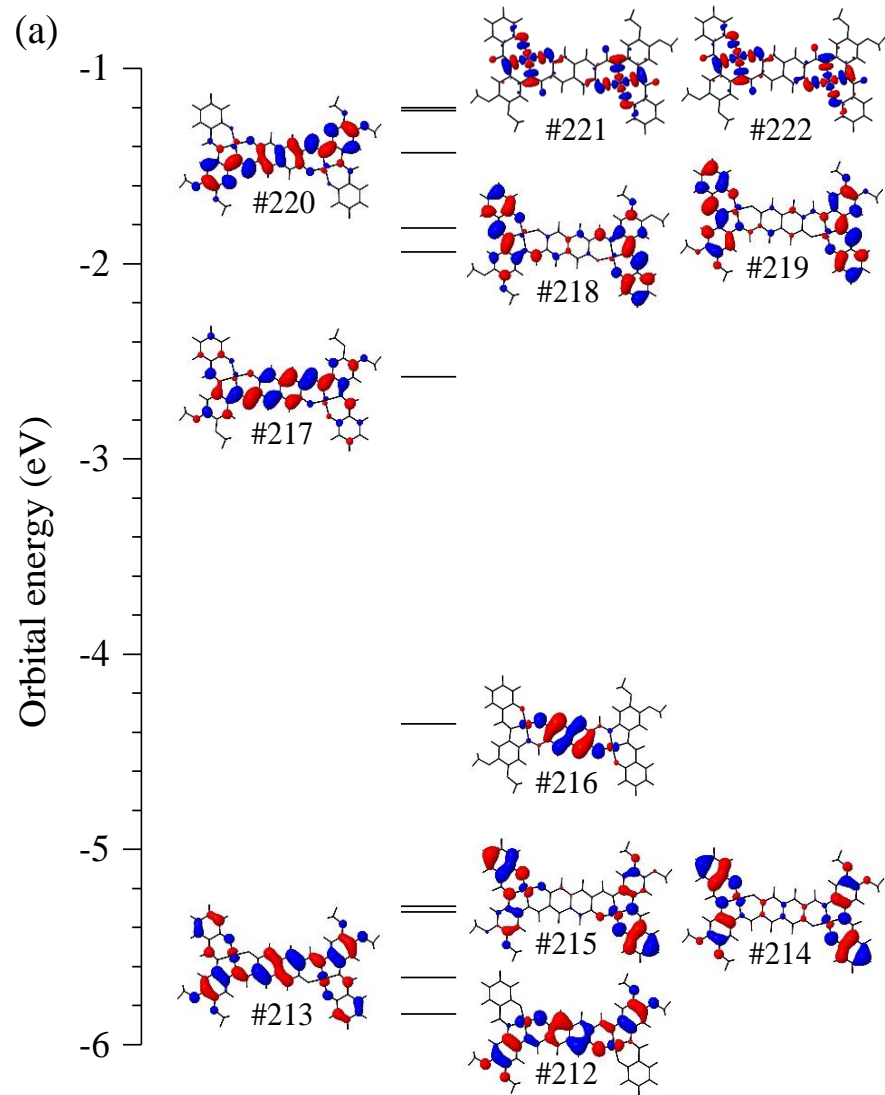
M_aM_b	Contributing Configurations	Contribution ^a	Assigned Transition	λ_{obsd} (nm)
Zn_2	No. 218 \rightarrow 219	0.50	$\pi \rightarrow \pi^*$ (naphthalene \rightarrow naphthalene)	703
	No. 217 \rightarrow 219	0.49	$\pi \rightarrow \pi^*$ (salphen \rightarrow naphthalene)	509sh, 475
	No. 215 \rightarrow 219	0.43	$\pi \rightarrow \pi^*$ (naphthalene \rightarrow naphthalene)	410
	{ No. 217 \rightarrow 221 No. 216 \rightarrow 220 }	0.23	$\pi \rightarrow \pi^*$ (salphen \rightarrow salphen)	
		0.17		
Ni_2	No. 216 \rightarrow 217	0.50	$\pi \rightarrow \pi^*$ (naphthalene \rightarrow naphthalene)	809
	No. 215 \rightarrow 217	0.41	$\pi \rightarrow \pi^*$ (salphen \rightarrow naphthalene)	550sh, 497sh
	No. 213 \rightarrow 217	0.47	$\pi \rightarrow \pi^*$ (naphthalene \rightarrow naphthalene)	432
NiZn	No. 217 \rightarrow 218	0.50	$\pi \rightarrow \pi^*$ (naphthalene \rightarrow naphthalene)	758
	No. 215 \rightarrow 218	0.47	$\pi \rightarrow \pi^*$ (Zn-salphen \rightarrow naphthalene)	524sh, 486sh
	No. 214 \rightarrow 218	0.42	$\pi \rightarrow \pi^*$ (Ni-salphen + naphthalene \rightarrow naphthalene)	424
	No. 213 \rightarrow 218	0.29	$\pi \rightarrow \pi^*$ (Zn-salphen + naphthalene \rightarrow naphthalene)	424

Abbreviation: TD-DFT, time-dependent density functional theory.

^aSquared coefficient for each electronic configuration.







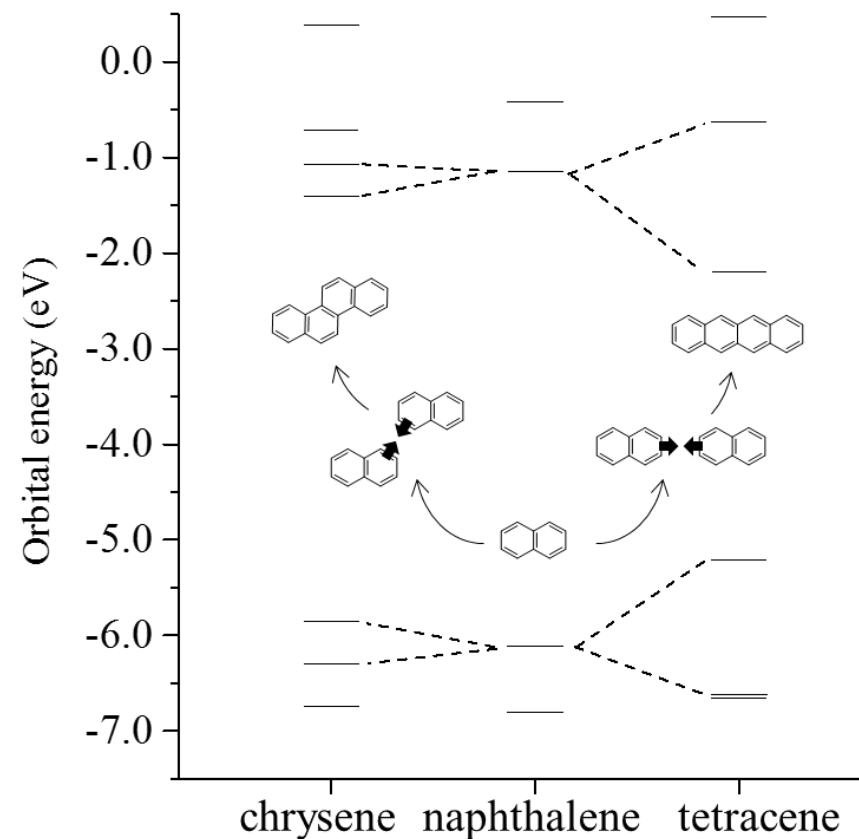
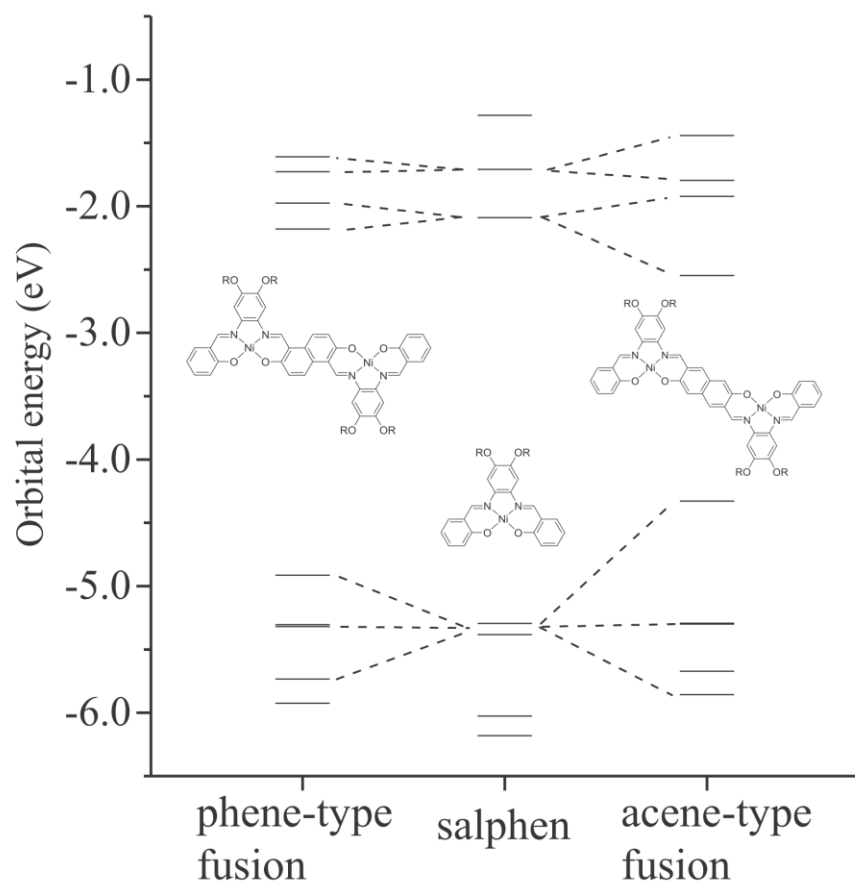
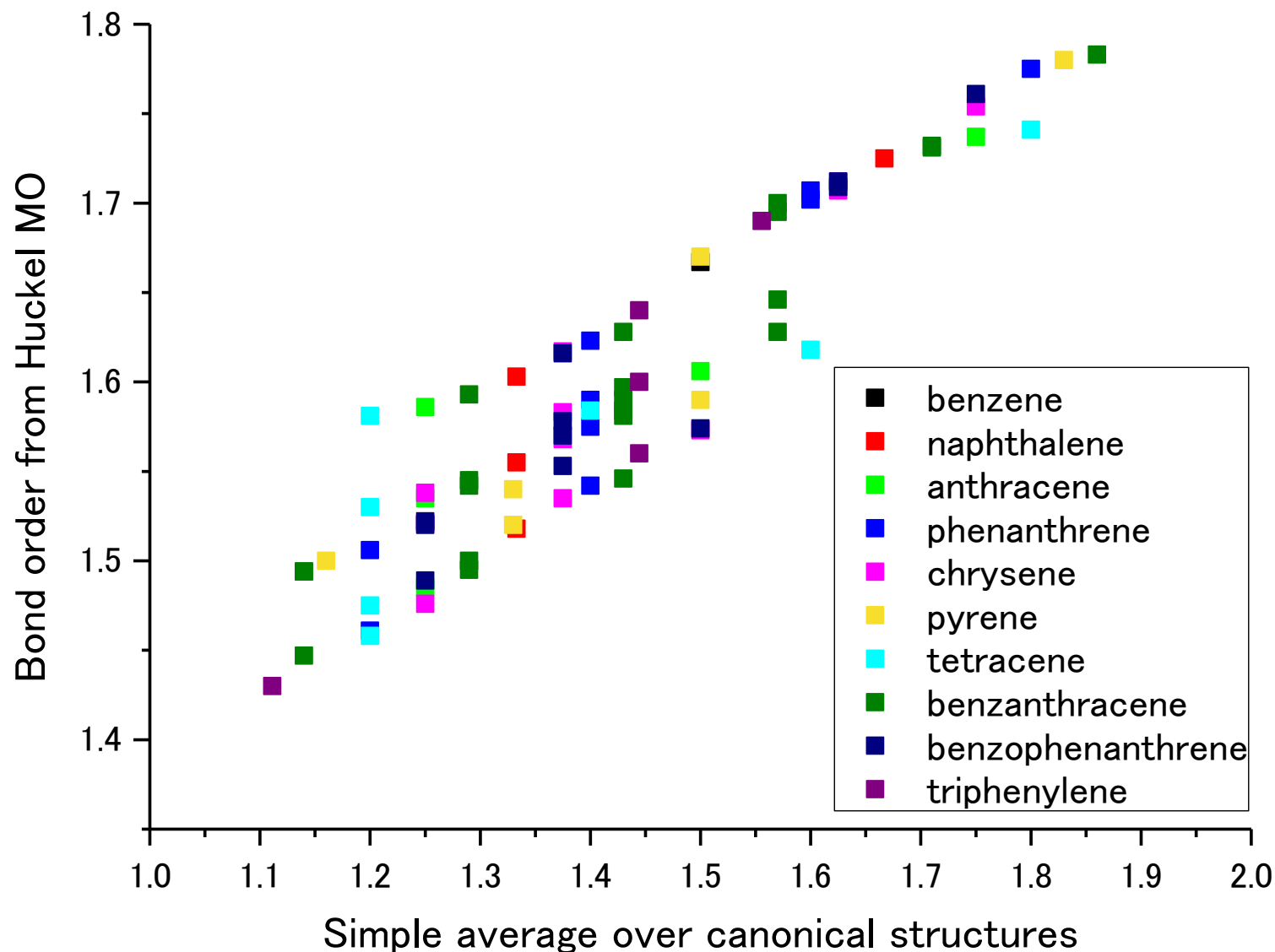


FIGURE 5 Comparison of the orbital energies of phenyl-type $\text{Ni}_2\text{L}^\alpha$, acene-type $\text{Ni}_2\text{L}^\beta$, and mononuclear **5**-Ni complexes. The dotted lines indicate that a certain orbital of a dinuclear complex is represented by a symmetrical or antisymmetrical combination of an orbital of the mononuclear complex

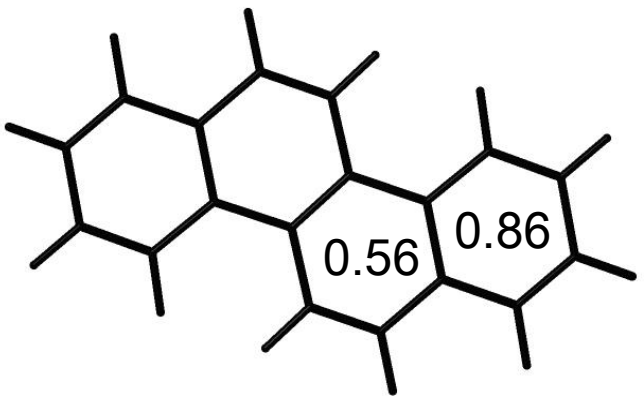
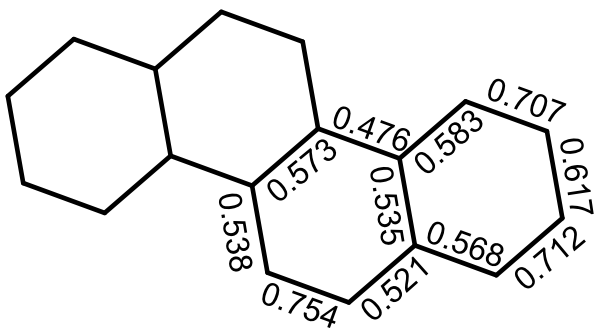
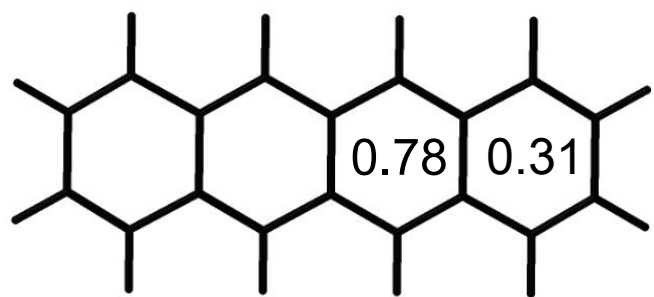
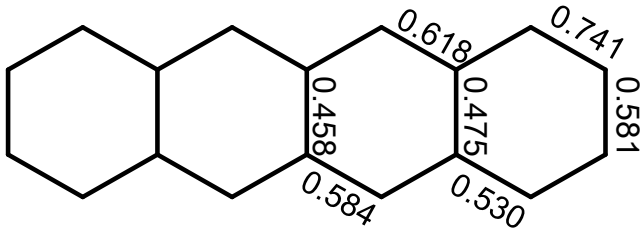
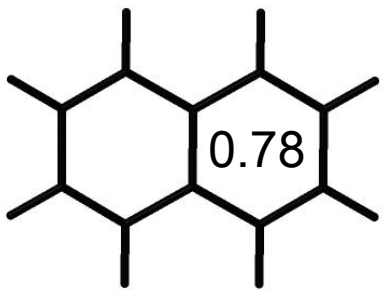
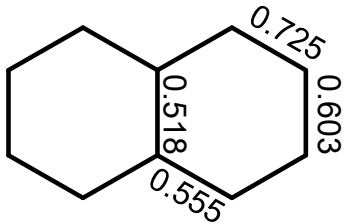
Figure S9 Comparison of the orbital energies of chrysene, tetracene and naphthalene. The dotted lines indicate that a certain orbital of a four-ring system is represented by a symmetrical or anti-symmetrical combination of an orbital of naphthalene.

結合次数の比較

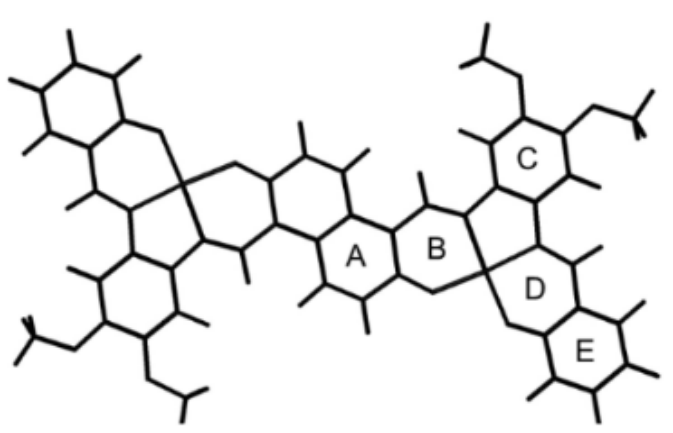
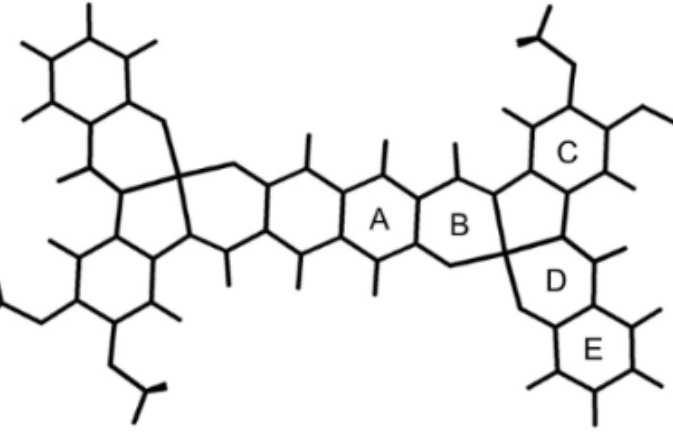
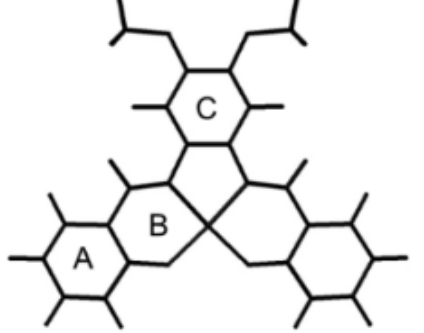
極限構造の単純平均とHückel法による計算値



HOMA、結合次数、共鳴安定化エネルギーの比較

(a)		 0.476, 0.583, 0.707, 0.617, 0.712, 0.568, 0.521, 0.754, 0.538, 0.573, 0.535	-7.19 β
(b)		 0.618, 0.741, 0.581, 0.530, 0.475, 0.458, 0.584	-6.93 β
(c)		 0.725, 0.603, 0.518, 0.555	-3.68 β
HOMA (HF/6-311G**)		Hückel bond order	ΔE_{res}

HOMA, NICS(0), NICS(1), NICS(1)_{zz}の比較

		HOMA	NICS(0)	NICS(1)	NICS(1) _{zz}
(a)		Ni ₂ L ^a			
	A	0.47	-4.0	-6.7	-13.8
	B	0.82	-5.9	-1.9	-3.7
	C	0.93	-9.3	-9.1	-19.5
	D	0.78	-6.1	-1.4	-3.5
	E	0.76	-5.4	-7.7	-18.1
(b)		Ni ₂ L ^b			
	A	0.77	-6.5	-8.6	-19.3
	B	0.64	-6.5	-1.5	-2.7
	C	0.92	-9.1	-9.1	-19.3
	D	0.81	-5.5	-1.4	-2.7
	E	0.72	-4.9	-7.3	-17.1
(c)		5-Ni			
	A	0.79	-5.3	-7.7	-18.3
	B	0.85	-6.0	-2.0	-3.9
	C	0.94	-9.6	-9.3	-20.1